Detailed Analysis of the Impact of the Code Doppler on the Acquisition Performance of New GNSS Signals

Myriam Foucras, Olivier Julien, Christophe Macabiau, Bertrand Ekambi

Detailed Analysis of the Impact of the Code Doppler on the Acquisition Performance of New GNSS Signals

Myriam FOUCRAS, ABBIA GNSS Technologies / ENAC, France
Olivier JULIEN, Christophe MACABIAU, ENAC, France
Bertrand EKAMBI, ABBIA GNSS Technologies, France

BIOGRAPHIES

Myriam FOUCRAS received her Masters in Mathematical engineering and Fundamental Mathematics from University of Toulouse in 2009 and 2010. Since 2011, she is a PhD. student at the Signal Processing and Navigation research group of the TELECOM laboratory of ENAC (Ecole Nationale de l'Aviation Civile). Her work is funded by ABBIA GNSS Technologies, in Toulouse, France working on the development of a GPS/Galileo software receiver.

Olivier JULIEN is the head of the Signal Processing and Navigation (SIGNAV) research group of the TELECOM laboratory of ENAC, in Toulouse, France. His research interests are GNSS receiver design, GNSS multipath and interference mitigation and GNSS interoperability. He received his engineer degree in 2001 in digital communications from ENAC and his PhD in 2005 from the Department of Geomatics Engineering of the University of Calgary, Canada.

Christophe MACABIAU graduated as an electronics engineer in 1992 from the ENAC in Toulouse, France. Since 1994, he has been working on the application of satellite navigation techniques to civil aviation. He received his PhD in 1997 and has been in charge of the TELECOM laboratory of the ENAC since 2011.

Bertrand EKAMBI graduated by a Master in Mathematical Engineering in 1999. Since 2000, he is involved in the main European GNSS projects: EGNOS and Galileo. He is the founder manager of ABBIA GNSS Technologies, a French SME working on Space Industry, based in Toulouse, France.

ABSTRACT

For several tens of years, when the main acquired signal was GPS L1 C/A and under normal circumstances, many results were derived assuming that there is no change in the received code frequency due to the incoming Doppler frequency. Nevertheless, [1] and [2] investigated the effect of the resulting code phase sliding during the correlation process and showed that the acquisition performance can significantly be degraded. Considering the new challenges (new environments and new modulations, signal structures, longer codes, faster code rate, and so on), this investigation needs to be reviewed. In this paper, the authors want to present some results dealing with the code Doppler effect on acquisition performances for several new GNSS signals.

INTRODUCTION

The number of transmitted GNSS (Global Navigation Satellite Systems) signals has significantly increased with the ongoing deployment of Galileo and Beidou constellations, the maintenance of GLONASS and the modernization of GPS. In order to share the same Lower band (L-band), the properties of these new GNSS signals were adapted. The main points of design and characterization of GNSS signals are:

- The carrier frequency f_L
- The spreading codes characterized by their length N, code frequency f_c also called chipping rate and which is the number of chips transmitted in 1 second and repetition period to improve autocorrelation and cross-correlation properties
- The modulation
    - BPSK (Binary Phase Shift Keying)
    - QPSK (Quadrature Phase Shift Keying)
    - CBOC (Composite Binary Offset Carrier)
    - TMBOC (Time Multiplexing Binary Offset Carrier)
    - …

GNSS applications based on high sensitivity and weak signals acquisition have become the most popular research areas [3]. The acquisition process in these degraded conditions requires large total integration time (through coherent and/or non-coherent accumulations) to accumulate signal energy.

The Doppler frequency, mainly caused by the satellite motion and the local oscillator [4], impacts twice the emitted signal: by modifying the central frequency (change estimated by the acquisition process) and by modifying the code frequency, resulting in a code Doppler. If the incoming Doppler frequency is small, the code Doppler can be ignored. However, in high Doppler conditions, it can be significant. Indeed, the code Doppler leads to change the spreading code period (reduced or expanded). For instance, for an incoming Doppler frequency of 10 kHz, it translates into one spreading code chip slip in 154 ms for GPS L1 C/A and for the same Doppler frequency, the 1 chip slip occurs in only 12 ms

for GPS L5. In this study, the Doppler frequency is assumed to be constant over the total integration time because the average rate of magnitude change of the Doppler frequency is less than 1Hz per second [4]

If the receiver does not take the code Doppler into account during the acquisition phase (which is the general case), this can result in degraded correlator outputs that will degrade the acquisition capability of the receiver.
It is thus relevant to discuss the code Doppler effect on GNSS acquisition performance:

- Degradations on the acquisition performance in terms of probability of detection if code Doppler is not compensated by the receiver
- Development of code Doppler compensation methods

This paper specifically focuses on by providing a mathematical study and some innovative results for widely used new signals. The motivation behind this investigation is to give careful instructions concerning the acquisition of GNSS signals and in particular in low C/N_0 environments. The accurate knowledge of the code Doppler impact on acquisition allows adapting and improving acquisition methods.
This paper is divided as follows:

- A first section serves as establishing the basis by presenting the considered GNSS signals, acquisition process and code Doppler problem leading to the problematic of the paper
- A second section develops the mathematical model of the distorted autocorrelation when considering a received signal affected by code Doppler and a local one
- Then, simulation results are presenting in the third section leading to the comparison of coherent/non-coherent accumulation methods and signals
- A fourth section is dedicated to the state-of-the-art of code Doppler compensation methods
- At the end, the conclusion will summarize the main results and present future works

I. ACQUISITION AND CODE DOPPLER

GNSS Signals

Several GNSS signals are considered in this study. They encompass most of the GPS and Galileo civil signals: GPS L1 C/A, L1C, L5 and Galileo E1 OS and E5 whose frequency plans are presented in Figure 1.

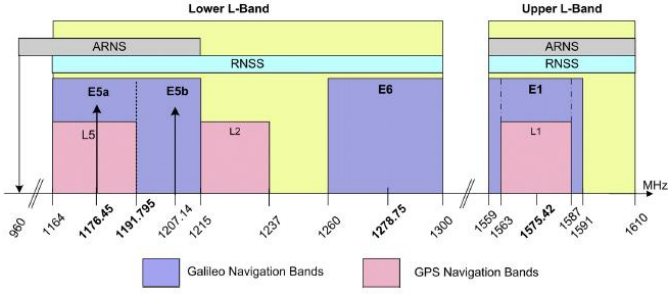

Figure 1: GPS and Galileo frequency plans [5]

In order to develop the code Doppler study and bot being dependent from other facts degrading acquisition performance, some assumptions on the considered GNSS signals are taken. Because the code Doppler impact on the acquisition is similar on both components (for composite signals) and without loss of generalities, only results on one component are presented (data component). Moreover, the data sequence and secondary code are supposed to be constants to 1 to avoid degradations due to bit transitions [6].
Table I gives a brief overview of the data component signal features; [7] and the Interface Control Documents are reference documents for more details: [8], [9], [10] and [5] for GPS L1C/A, L1C, L5 and Galileo E1/E5 respectively.

Table I: Data component signal features

Signal		Modulation	Central frequency (MHz)	Code frequency (MHz)
GPS L1 C/A		BPSK	1575.42	1.023
GPS L1C-D		BOC	1575.42	1.023
GPS L5-D		BPSK	1176.45	10.23
Galileo E1 OS-B		CBOC (6,1,1/11)	1575.42	1.023
Galileo E5	a-I	BPSK	1176.45	10.23
	b-I	BPSK	1207.14	10.23

The data component of the received GNSS signal can be represented as follows over a time interval with constant Doppler:

$$r(t-\tau) = Ad(t-\tau)c_2(t-\tau)c(t-\tau)p(t-\tau) \times \cos(2\pi(f_L + f_d)t + \phi_0) + n(t) \quad (1)$$

Where:

- A is the signal amplitude
- d is the data sequence
- c_2 is the secondary code (NH_{10}) for GPS L5
- c is the spreading code (PRN) periodic then $c(N+i) = c(i)$ for all $i = 1 \dots N$
- f_d is the incoming Doppler frequency whose uncertainty space is $[-10; 10]$ kHz
- τ is the incoming code delay
- ϕ_0 is the initial phase of the incoming signal at the beginning of the time interval T_0
- n is the incoming noise which is assumed to be a centered Gaussian distribution white noise with a constant two-sided power spectral density equal to N_0
- p is the resulting subcarrier for BOC-modulated signals, if any, using:

$$p_{BOC(x)}(t) = sign(\sin(2\pi \times xf_0 \times t)) \quad (2)$$

Table II focuses on the spreading code properties for the data component to complete the previous signal expression. The spreading code chips number is denoted by N and the spreading code chip duration T_c leading to a spreading code period equal to NT_c.

Table II: PRN codes properties on the data component

Signal		PRN length (chips)	PRN period (ms)	Subcarrier p
GPS L1 C/A		1023	1	None
GPS L1C-D		10230	10	$p_{BOC(1)}(t)$
GPS L5-D		10230	1	None
Galileo E1 OS B		4092	4	$\frac{\sqrt{10}p_{BOC(1)}(t)+p_{BOC(6)}(t)}{\sqrt{11}}$
Galileo E5	a-I	10230	1	None
	b-I	10230	1	None

Assuming the modulation of Galileo E5 a-I as a BPSK, only results on GPS L5 are presented because the Galileo E5a/b-I signal has the same characteristics as the GPS L5 signal so what is true for GPS L5 is also valid for Galileo E5a-I.

Acquisition

At the receiver level, through a correlation process as depicted in Figure 2, the acquisition process consists in giving a rough estimation of the incoming signal parameters.

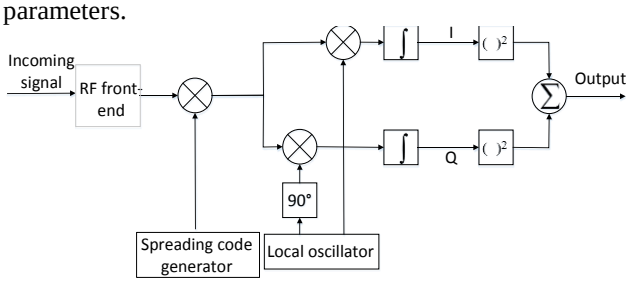

Figure 2: Acquisition process scheme

At the end, the in-phase $I(k)$ and quadrature $Q(k)$ correlator outputs, resulting of the correlation process, are expressed by:

$$\begin{cases} I(k) = n_I(t) + \frac{A}{2}R(\varepsilon_\tau)\times \\ \cos\left(2\pi\varepsilon_f\left(T_0 + \left(k+\frac{1}{2}\right)T_I\right) + \phi_0\right) sinc(\pi\varepsilon_f T_I) \\ Q(k) = n_Q(t) + \frac{A}{2}R(\varepsilon_\tau)\times \\ \sin\left(2\pi\varepsilon_f\left(T_0 + \left(k+\frac{1}{2}\right)T_I\right) + \phi_0\right) sinc(\pi\varepsilon_f T_I) \end{cases} \quad (3)$$

Where

- $\varepsilon_\tau = |\tau - \hat{\tau}|$ is the code delay error
- $\varepsilon_f = \left|f_d - \widehat{f_d}\right|$ is the Doppler frequency error
- n_I and n_Q are the noise at the correlator output which follows a centered Gaussian distribution and their variances are $\sigma^2 = \frac{N_0}{4T_I}$ [11]
- $[T_0 + kT_I;\ T_0 + (k+1)T_I]$ is the integration interval beginning at T_0 and lasting T_I
- $R(.)$ is the autocorrelation function of the spreading code defined by:

$$R(\tau) = \frac{1}{N}\sum_{i=1}^{N}\big(c(i)p(i)\big)\big(c(i-\tau)p(i-\tau)\big) \quad (4)$$

Figure 3 presents the autocorrelation functions for all of the considered GNSS signals. For BOC-modulated signals (Galileo E1 OS and GPS L1C), the autocorrelation function is sharpest than
BPSK-modulated signals (GPS L1 C/A and GPS L5).

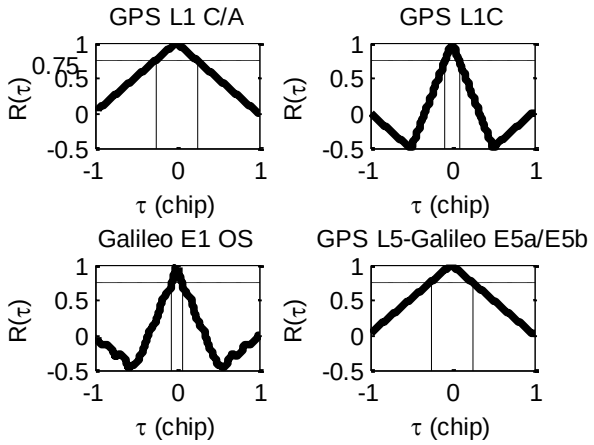

Figure 3: Autocorrelation functions

A classical acquisition method, the serial search acquisition method is based on an acquisition grid which covers the frequency and time uncertainty search space. Then, the incoming signal is correlated with a locally generated one which the estimation parameters couple $(\widehat{f_d}, \hat{\tau})$ is read one by one in the acquisition grid. It is quite clear that a trade-off should be chosen between the search space discretization and the acquisition execution time (in general wanted as short as possible).
We decide, as it is done in [12], that the total maximal degradations due to the discretization acquisition grid should be lower than 3.4 dB (2.5 dB in the time space and 0.9 in the frequency space). This determines the width of a bin in the acquisition grid in the frequency and time dimension by assuming uniform distributions. If only 2.5 dB losses are accepted in the time domain (equivalent to $R(\varepsilon_\tau) \geq 0.75$) then the bin width for the code delay should be lesser than:

- $2 \times \frac{1}{4}$ for BPSK-modulated signals
- 2×0.0833 for GPS L1C
- 2×0.0593 for Galileo E1 OS

In general, to evaluate the acquisition process, two criteria are used: the mean acquisition time and the probability of detection which is the probability to correctly acquire the signal under some conditions (sensitivity, integration time…). Herein, because we want to evaluate the degradations on the detection capability due to the code Doppler, we focus on the probability of detection.
To determine it, a detection hypothesis test is applied based on Neyman-Pearson's approach [13]:

- The null hypothesis H_0 assumes that the useful signal is not present (or its parameters are not well estimated), in other words, there is only noise
- The alternative hypothesis H_1 assumes that the useful signal is present and its parameters are correctly recovered

The acquisition detector is:

$$T(k) = I^2(k) + Q^2(k) = \frac{A^2}{4}R^2(\varepsilon_\tau)sinc^2(\pi\varepsilon_f T_I) + n_I^2(t) + n_Q^2(t) \quad (5)$$

The acquisition test becomes:

$$H_0: T < T_h \text{ against } H_1: T \geq T_h \quad (6)$$

Where T_h is the acquisition threshold

Knowing the probability of false alarm and fixed at $P_{fa} = 10^{-3}$, the threshold T_h can be easily determined:

$$P_{fa} = P_{H_0}\left(\frac{T_{H_0}(k)}{\sqrt{\sigma^2}} > \frac{T_h}{\sqrt{\sigma^2}}\right) = 1 - F_{\chi^2(2)}\left(\frac{T_h}{\sqrt{\sigma^2}}\right) \quad (7)$$

The normalized acquisition detector under the null hypothesis T_{H_0} is a chi-square distribution because it has the distribution of $\left(n_I^2(t) + n_Q^2(t)\right)/\sigma^2$. Two squared centered Gaussian distribution are summed then the number of degrees of freedom is 2.

Then, the probability of detection, the probability that the acquisition detector under the alternative hypothesis H_1, T_{H_1}, exceeds the threshold T_h is:

$$P_d = P_{H_1}\left(\frac{T_{H_1}(k)}{\sqrt{\sigma^2}} > \frac{T_h}{\sqrt{\sigma^2}}\right) = 1 - F_{\chi^2(2,\lambda)}\left(\frac{T_h}{\sqrt{\sigma^2}}\right) \quad (8)$$

Where λ is the non-centrality parameter equal to:

$$\lambda = \frac{A^2}{N_0}T_I R^2(\varepsilon_\tau)sinc^2(\pi\varepsilon_f T_I) \quad (9)$$

The integration time T_I is chosen to be a multiple of the spreading code period (NT_c) and in general it is one. But in low SNR environment, signal acquisition cannot be successful in one spreading code period. Then, to reach higher probabilities of detection and acquisition sensitivity, it is possible to increase the total integration time (that means more than one spreading code period should be accumulated). Commonly used methods are the coherent integration and non-coherent summations. In both cases, the total integration time is K spreading code periods. In general, the data bit transition is one of the main factors that limit the integration time but in the context of this paper, as previously said, we assume that there is no data.

1) Non-coherent integration

Successive correlator outputs on the spreading code period are non-coherently summed; for K non-coherent summations on the spreading code period NT_c, the acquisition detector (5) becomes:

$$T_K = \sum_{k=1}^{K}\left(I^2(k) + Q^2(k)\right) \quad (10)$$

In this case, the number of degrees of freedom of the chi-square distribution under H_0 and H_1 is $2K$.

2) Coherent integration

Only one integration is done but on $K \times NT_c$. Then, the coherent integration interval as defined in (3) becomes:

$$[T_0 + kT_I;\ T_0 + (k+K)T_I] \quad (11)$$

The distribution of the acquisition detector is a chi-square with 2 degrees of freedom.

To only study the acquisition degradation due to code Doppler, we assume that the incoming Doppler frequency and phase are well estimated. Moreover, the code delay is supposed to be null at the beginning of the correlation process; that means that the residual code delay error is only induced by code Doppler.

To speed up the acquisition process, the Fourier transform is often used [14]. In this way, for a given Doppler frequency estimate $\hat{f_d}$, the correlator outputs for all of the code delay estimates $\hat{\tau}$ are computed in the same time. The results on acquisition performances obtained with Matlab use Fourier transform.

Code Doppler

The code Doppler, noted f_{cd}, is the code frequency derived from the incoming Doppler shift [15]. As it is defined in (12), it depends on:

- The incoming Doppler frequency f_d
- The L-band central frequency f_L
- The code frequency f_c

$$f_{cd} = f_c \times \frac{f_L + f_d}{f_L} \Leftrightarrow T_{cd} = T_c \times \frac{f_L}{f_L + f_d} \quad (12)$$

Where $T_x = 1/f_x$ is the chip duration.

T_c is a priori known because it refers to the local spreading code whereas T_{cd} is unknown.

The difference in code frequency leads to a change in the spreading code period as it can be seen in Figure 4 where 3 periods of a 4-chips spreading code are represented:

- A positive code Doppler frequency causes the spreading code duration to shrink ($T_{cd} < T_c$)
- A negative Doppler shift causes the spreading code duration to expand ($T_{cd} > T_c$)

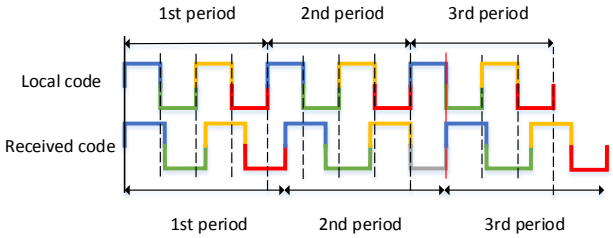

Figure 4: Code Doppler effect on the spreading code period

Mathematically, it can be modeled as two ways. The first one which is used to derive the mathematical model uses the rectangular function:

$$\sum_{i=1}^{N} c(i).rect\left(\frac{t}{T_{cd}} - i\right) \quad (13)$$

Where

- $c(i)$ is the spreading code chip value
- $rect\left(\frac{t}{T_{cd}}\right) = \begin{cases} 1, 0 \leq t \leq T_{cd} \\ 0, otherwise \end{cases}$ is the rectangular function

The other way, which is used in [3], [16] and [17], consists in introducing the fractional perturbation caused by Doppler frequency and noted $\eta = f_d/f_L$:

$$c\left((1+\eta)(t-i)\right) \quad (14)$$

As it will be shown, the main effects of the code Doppler are degradation in the magnitude of the autocorrelation function and a shift of the true code delay. If the shift between the received spreading code and the local

spreading code (without Doppler) exceeds 1 chip then the correlation process (summation) no longer makes sense because the power of the signal cannot be accumulated. This obvious limit of 1 chip represents the loss of matching between the two sequences. The maximum total integration time before the slip of 1 chip depending on the incoming Doppler frequency and GNSS signal, is given in Table III.

Table III: Offset of 1 chip depending on the incoming Doppler frequency

	Incoming Doppler frequency Offset of 1 chip (ms) Offset of 1 chip (number of spreading code periods)				
Signal	**2 kHz**	**4 kHz**	**6 kHz**	**8 kHz**	**10 kHz**
GPS L1 C/A	770 770	385 385	257 257	193 193	154 154
GPS L1C-D	770 77	385 38.5	257 25.7	193 19.3	154 15.4
GPS L5-D	58 58	29 29	20 20	15 15	12 12
Galileo E1 OS B	770 192.5	385 96.25	257 64.25	193 48.25	154 38.5
Galileo E5a-I	58 58	29 29	20 20	15 15	12 12

For example, let us assume an incoming Doppler frequency of 10 kHz, for the GPS L1 C/A signal, this leads to a code Doppler of $f_{cd} = 1.023e^{6} - 6.49$ Hz. Then, a chip offset occurs after 154 ms; equivalent to 154 spreading code periods. However, for the L5 signals, a chip offset appears after 12 ms (12 spreading code periods). One can celarly understand that in 12 ms, it seems to be difficult to acquire weak signals because the total integration time is too short. Even for low Doppler frequencies (the incoming Doppler is lower for L5 signals rather than L1 signals), the total integration time is short. The slip in chip in one spreading code period is presented in Figure 5.

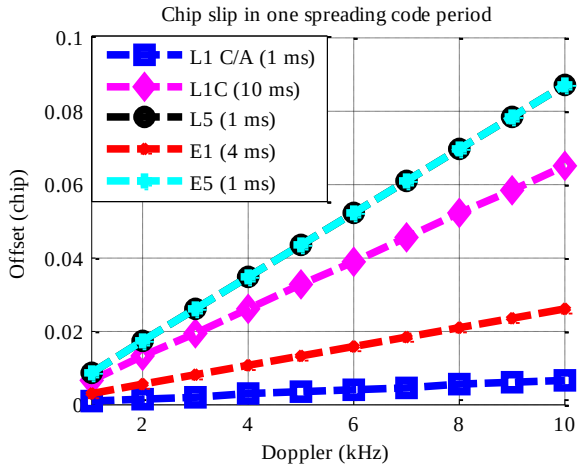

Figure 5: Chip offset in one spreading code period

This first result highlights the limits on the total integration time when several spreading code periods are required to acquire signals without Doppler compensation algorithms.

Moreover, it is worth noting that the code Doppler impact is visible on the first spreading code due to the use of high sampling frequency.

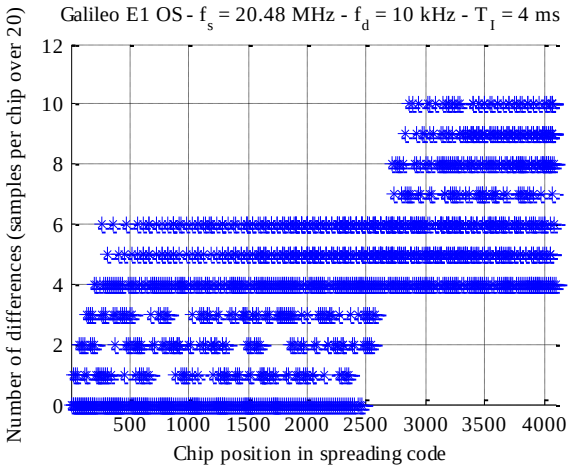

Figure 6: Differences number of samples per chip

For example, for a sampling frequency of $f_s = 20.48$ MHz let us simulate the first Galileo E1 OS spreading code (with a CBOC modulation) with no Doppler on the one hand and on the other hand with an incoming Doppler frequency of 10 kHz. Figure 6 presents the number of sample slips per chip for each chip in the first spreading code. For the last chips, around one half of the samples are slipped. Over the first spreading code, there are around 14000 differences over the 81920 samples (17%) even if the chip offset after one spreading code period is lesser than 1 sample ($4 \times \frac{1}{154} = 0.026$ chip corresponds to 0.52 sample).

This section presented the problem that is addressed in this paper: the impact of the code Doppler on the acquisition performance. In the next sections, a simple mathematical model is given with some results.

II. MATHEMATICAL ANALYSIS

Mathematical model of distorted autocorrelation

To simplify and be able to develop the mathematical model of autocorrelation function, some assumptions need to be taken:

- There is no BOC subcarrier, then the values taken by the spreading code sequence are 1 or -1
- There is no incoming code delay, this means that $\tau = \hat{\tau} = 0$ and there is no a chip offset at the beginning of the autocorrelation process due to code Doppler

We precise that if $b \geq a$ then $1_{[b;a]}(t) = 0$ and $\int 1_{[a;b]}(t)dt = b - a$

In this section, we focus on the autocorrelation function when the incoming spreading code c_r is affected by the Doppler. Then, it can be written as:

$$c_r(t) = \sum_{j=1}^{N} c(j) rect\left(\frac{t}{T_{cd}} - j\right) \quad (15)$$

In the same way, the local spreading code c_l is:

$$c_l(t) = \sum_{i=1}^{N} c(i) rect\left(\frac{t}{T_c} - i\right) \quad (16)$$

Then, on the integration interval $[kNT_c; (k+1)NT_c]$, the autocorrelation function affected by the code Doppler $\tilde{R}(k)$ is given by (19) which is obtained by dividing the total integration interval in small integration intervals where the local spreading code chip is constant. Then, as it is done in (20), the product of the rectangular functions can be seen as an indicator function $1_{[\max((i-1)T_c;(j-1)T_{cd});\min(iT_c;jT_{cd})]}$. Applying (20) to (19) gives (21) which can be simplified by (22). The double sum (on i and on j) can be seen as the sum on i of three terms. To be more precise, as it is depicted in Figure 7, the chip i of the local sequence can be multiplied by the chips $j = i$ or $j = i + 1$ of the received spreading code.

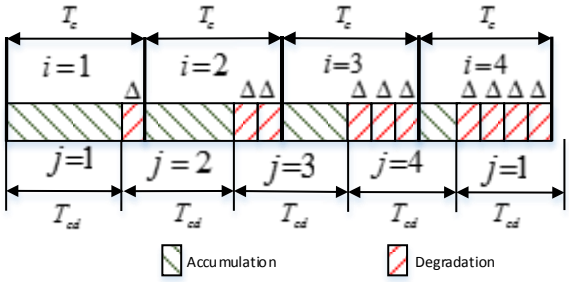

Figure 7: Correlation process with different code frequencies

Then, by noting $\Delta = |T_c - T_{cd}|$ the absolute difference between the duration of the local and the received spreading code chips, the general expression of the resulting autocorrelation function is given by (23). It is composed of two terms:

- $N \max(T_c, T_{cd}) - \Delta \frac{N(N+1)}{2}$ corresponds to cumulative sum (green zones) where the chips of the two sequences correspond
- $\Delta \sum_{i=1}^{N} i \left[c(i)c(i+1) \times 1_{[T_c > T_{cd}]} + c(i)c(i-1) \times 1_{[T_c < T_{cd}]}\right]$ corresponds to potential degradations (red zones) where the chips in the two spreading code sequences are not in the same position and their product result can be 1 or -1 with a probability of one half for each one

The result can be easily verified by simulations but it seems to be difficult to extend in a general case (for CBOC-modulated signals, with initial delay…)

Resulting autocorrelation function approximation

Matlab simulations were run to verify that the resulting autocorrelation function can be approximated by the autocorrelation function for different signals, here only the GPS L1 C/A approximation is shown. On the one hand, the resulting autocorrelation function is evaluated at each spreading code period:

$$\tilde{R}_0(k) = \frac{1}{N_s} \sum_{i=1}^{N_s} c_r(kNT_c + i) c_l(kNT_c + i) \quad (17)$$

Where:

- k corresponds to the integration period (for $k = 1$, we assume that the first chips of the received and local sequences are correctly synchronized)
- N_s is the number of samples in one local spreading code period
- $\tilde{R}_0(k)$ represents the affected autocorrelation function in 0 after $(k-1)$ local spreading code periods

On the other hand, the code delay is evaluated and the autocorrelation function taken in this point is calculated:

$$R(\tau) = 1 - |k \times N \times \Delta| \quad (18)$$

$$\begin{aligned} \tilde{R}(k) &= \frac{1}{NT_c} \int_{kNT_c}^{(k+1)NT_c} c_l(t) c_r(t) dt = \frac{1}{NT_c} \int_{kNT_c}^{(k+1)NT_c} \sum_{i=1}^{N} c(i) rect\left(\frac{t}{T_c} - i\right) \sum_{j=1}^{N} c(j) rect\left(\frac{t}{T_{cd}} - j\right) dt \\ &= \frac{1}{NT_c} \sum_{i=1}^{N} c(i) \sum_{j=1}^{N} c(j) \int_{kNT_c}^{kNT_c + iT_c} \sum_{j=1}^{N} c(j) rect\left(\frac{t}{T_c} - i\right) rect\left(\frac{t}{T_{cd}} - j\right) dt \end{aligned} \quad (19)$$

$$rect\left(\frac{t}{T_c} - i\right) rect\left(\frac{t}{T_{cd}} - j\right) = \begin{cases} 1, & if \begin{cases} (i-1)T_c \le t \le iT_c \\ (j-1)T_{cd} \le t \le jT_{cd} \end{cases} \\ 0, & otherwise \end{cases} = 1_{[\max((i-1)T_c;(j-1)T_{cd});\min(iT_c;jT_{cd})]}(t) \quad (20)$$

$$\tilde{R}(k) = \frac{1}{NT_c} \sum_{i=1}^{N} c(i) \sum_{j=1}^{N} c(j) \int_{kNT_c}^{kNT_c + iT_c} 1_{[\max((i-1)T_c;(j-1)T_{cd});\min(iT_c;jT_{cd})]}(t) dt \quad (21)$$

$$\begin{aligned} \tilde{R}(k) &= \frac{1}{NT_c} \sum_{i=1}^{N} (0 + c(i)c(i)[iT_{cd} - (i-1)T_c] + c(i)c(i+1)[iT_c - iT_{cd}]) \\ &= \frac{1}{NT_c} \left(NT_c + (T_{cd} - T_c) \frac{N(N+1)}{2} + (T_c - T_{cd}) \sum_{i=1}^{N} i\, c(i)c(i+1) \right) \end{aligned} \quad (22)$$

$$\tilde{R}(k) = \frac{1}{NT_c} \left(N \max(T_c, T_{cd}) - \Delta \frac{N(N+1)}{2} + \Delta \sum_{i=1}^{N} i \left[c(i)c(i+1) \times 1_{[T_c > T_{cd}]} + c(i)c(i-1) \times 1_{[T_c < T_{cd}]}\right] \right) \quad (23)$$

Figure 8 depicts the verification result for the GPS L1 C/A spreading code.

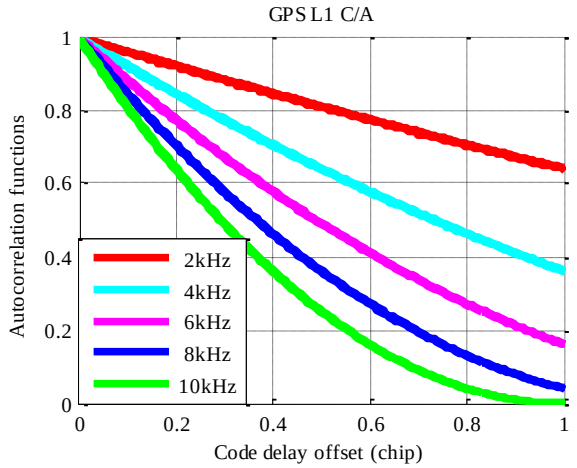

Figure 8: Approximation of the affected autocorrelation function

For all of the incoming Doppler frequencies, the two curves are superposed which means that

$$\tilde{R}_0(k) \approx R(k \times N \times \Delta) \quad (24)$$

III. SIMULATION RESULTS

In this section, some simulation results are presented to illustrate the code Doppler effect on the acquisition performance. The results based on the normalized squared autocorrelation function differ with the summation technique (coherent or non-coherent). Firstly, the non-coherent results are observed.

Non-coherent summations

Based on the total integration time before the slip of 1 chip (Table IV), the autocorrelation function affected by the code Doppler is presented in Figure 9. The black curve is the squared autocorrelation function without Doppler, the reference one and the worst case is for a Doppler of 10 kHz in green.

For the BPSK-modulated signals (GPS L1 C/A and GPS L5), the autocorrelation function shape becomes rounded and offset compared to the reference triangular. The amplitude of the maximum value is reduced and the peak is shifted to the right for a negative Doppler. For the BOC-modulated signals (GPS L1C and Galileo E1 OS), the secondary peaks which characterize the autocorrelation function tend to disappear leading to a flat curve.

For the same maximum total integration time (154 ms for Galileo E1 OS, GPS L1 C/A and L1C), the impact on the resulting autocorrelation function shape is different mainly due to the modulation. Table IV provides the characteristics of the main peak of the normalized autocorrelation for an incoming Doppler of 10 kHz. The peak slips of 1 bin in the acquisition grid for BPSK-modulated signal and because the peak is not evident for BOC-modulated signals, there is a change of 4 or more bins.

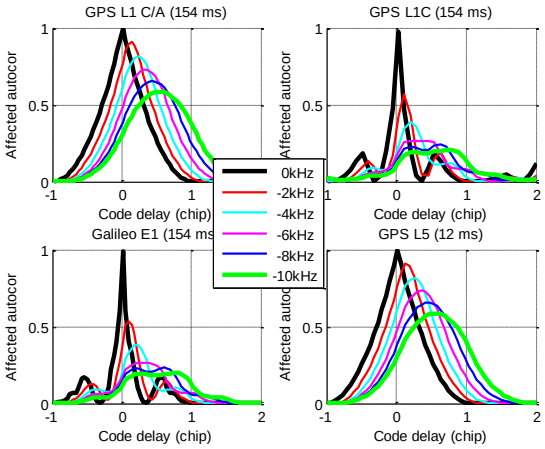

Figure 9: Affected autocorrelation function shape (Non-coherent)

Table IV: Main autocorrelation function peak for a 10 kHz incoming Doppler

	GPS L1 C/A	GPS L1C	Galileo E1 OS	GPS L5
K	154	15	38	12
Maximum amplitude	0.58	0.20	0.20	0.59
Argmax (chip)	0.54	0.67	0.75	0.56

Figure 10 provides the amplitude losses taken in the main peak versus the incoming Doppler frequency.

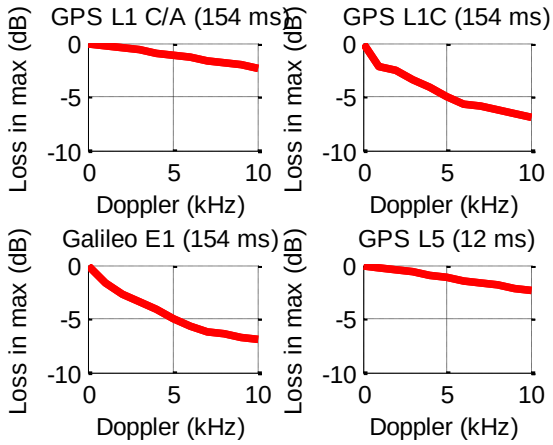

Figure 10: Losses on the autocorrelation function due to code Doppler (Non-coherent)

Due to the flattening of the autocorrelation function curve for BOC-modulated signals, losses in the main peak are higher (7 dB in the worst incoming Doppler frequency) than BPSK-modulated signals (2.4 dB). This means that for weak signals, the acquisition becomes very hard as it can be seen in Figure 11 with the probability of detection whose mathematical expression is given by (25) at 27 dB-Hz.

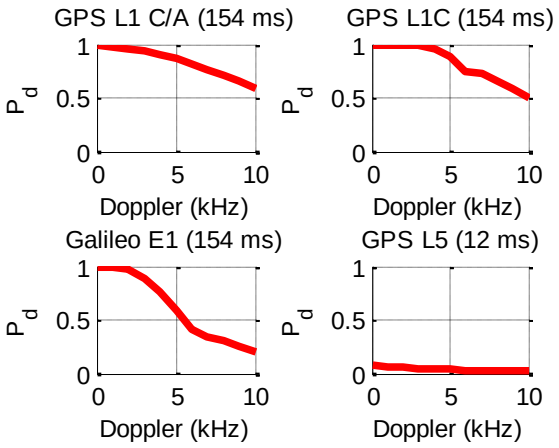

Figure 11: Probability of detection for weak signal and a non-coherent integration on the maximum allowed signal length

$$\begin{aligned} P_d &= 1 - F_{\chi^2(2K,\lambda)}\left(F^{-1}_{\chi^2_{2K}}(1-P_{fa})\right) \\ \lambda &= 2 \times \frac{C}{N_0} \times NT_c \times \max\left(\sum_{k=1}^{K}\left(\tilde{R}(k)\right)^2\right) \end{aligned} \quad (25)$$

For the GPS L1 signals, the probability of detection is equivalent even if there are more losses on the amplitude for the GPS L1C signals but it is compensated by longer coherent accumulation (on the spreading code period). For Galileo E1 OS, which has the same losses but a shorter spreading code period (4 ms instead of 10 ms), the probability of detection is close to 0.2 for high Doppler frequency (10 kHz). For GPS L5, the probability of detection is very low, this is explained by the very short integration time.

Coherent summations

Now, let us look at the coherent summation. The same incoming and local signals are processed but in a coherent way; this means that only one correlation on the total integration time is achieved.
As it was done in Figure 9, Figure 12 presents the autocorrelation function for the maximum integration time before a 1-chip offset for several incoming Doppler frequencies.

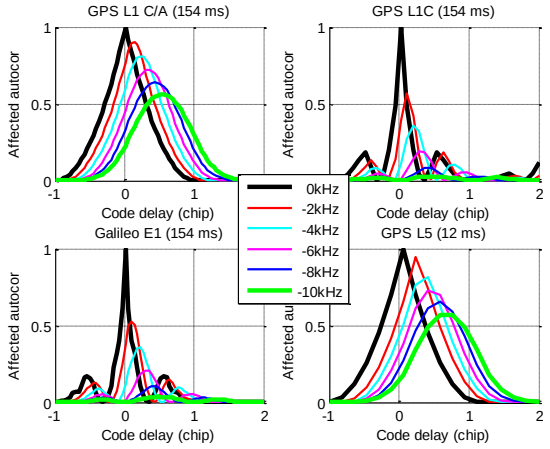

Figure 12: Affected autocorrelation function shape (Coherent)

For BPSK-modulated signals, the shape of the autocorrelation function seems to be similar as for non-coherent acquisition technique. However, for BOC-modulated signals, the flattening effect is very important leading to a quasi-null function for the worst case (in green). Indeed, Table V gives the amplitude of the peak of the resulting autocorrelation function. For the GPS L1C and Galileo E1 OS signals, the amplitude peak is around 0.035 which is lower than 0.2 for non-coherent acquisition technique (Table IV).

Table V: Main autocorrelation function peak for a 10 kHz incoming Doppler

	GPS L1 C/A	**GPS L1C**	**Galileo E1 OS**	**GPS L5**
KNT_c (ms)	154	154	154	12
Maximum amplitude	0.56	0.06	0.08	0.55
Argmax (chip)	0.5	0.46	0.46	0.54

The losses on the peak of the autocorrelation function for different coherent summations are presented in Figure 13 for the maximum total integration time. For the GPS L1 C/A and GPS L5 signals, the losses on the acquisition detector due to the code Doppler on the autocorrelation function (2.5 dB for 10 kHz) are similar that ones for non-coherent acquisition technique. As expected, the losses are important for the BOC-modulated signals (for 10 kHz more than 12 dB).

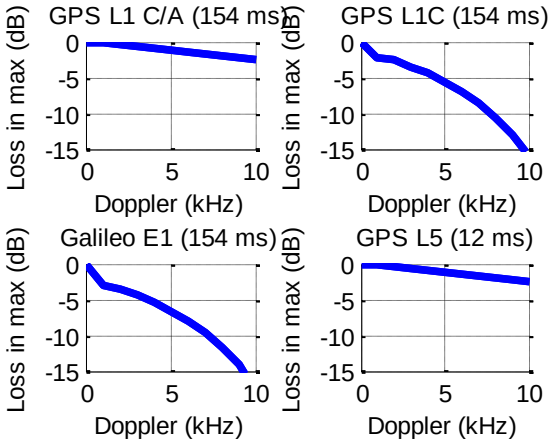

Figure 13: Losses on the autocorrelation function due to code Doppler (Coherent)

Knowing the losses in dB on the main peak of the resulting autocorrelation function, the probability of detection can be evaluated depending on the Doppler frequency; results are shown in Figure 14.

$$\begin{aligned} P_d &= 1 - F_{\chi^2(2,\lambda)}\left(F^{-1}_{\chi^2_2}(1-P_{fa})\right) \\ \lambda &= 2\frac{C}{N_0} \times KNT_c \times \max\left(\left(\tilde{R}_0\right)^2\right) \end{aligned} \quad (26)$$

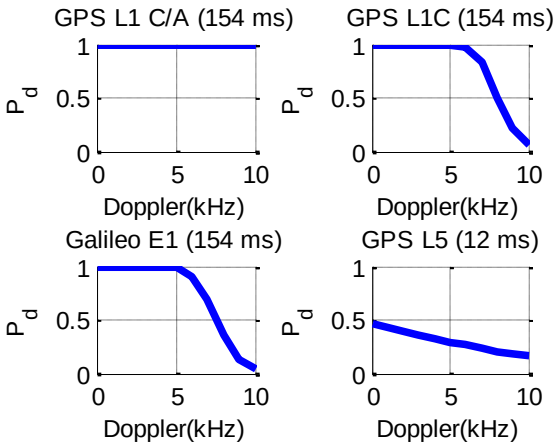

Figure 14: Probability of detection for weak signal and a coherent integration on the maximum allowed signal length

When not considering data sequence presence, it is preferable to coherently integrate rather than non-coherently sum for the same total integration time [18]. Then, the probability of detection in presence of code Doppler is still better for coherent summation than non-coherent summation. Let us note for the GPS L1 C/A signal, the probability of detection seems to be not affected by code Doppler due to the long coherent integration time.

Discussion

To complete the coherent accumulation results, we present in Figure 15 the probability of detection in function of the received sensitivity for Galileo E1 OS on 80 ms (coherently accumulation). It is more degraded for low C/N_0 than high C/N_0 and it is really accentuated for high incoming Doppler frequency. Then, we will interest on the impact of the code Doppler for low C/N_0.

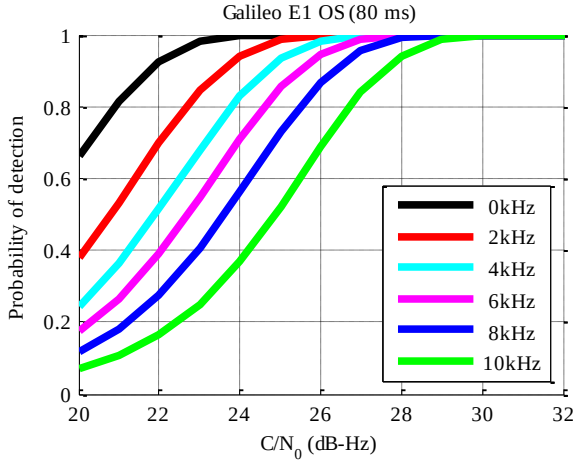

Figure 15: Probability of detection for different Doppler versus the sensitivity

Without Doppler, it is interesting to assess the minimum integration time so that the receiver can acquire a signal with a target C/N0 and a target probability of detection. This is shown in Figure 16 in the case of a signal with a C/N0 of 27 dB•Hz - on the data component for composite signals (GPS L1C, Galileo E1 OS and GPS L5) or total signal for GPS L1 C/A.

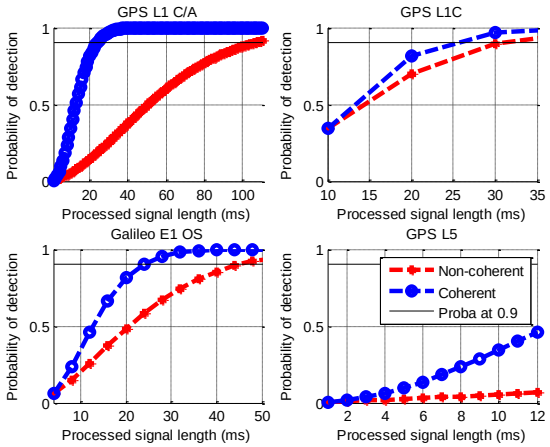

Figure 16: Required acquisition time to reach a high probability of detection without considering Doppler for weak signals (27 dB•Hz)

To complete Figure 16, Table VI provides the required time to acquire a signal at 27 dB•Hz with a high probability (90%) and without Doppler. This corresponds to the intersection of the red and blue curves with the black horizontal line materializing a probability of detection of 0.9.

Table VI: Required integration time for a probability of detection greater than 0.9 and a C/N_0 of 27 dB•Hz (without Doppler)

	GPS L1 C/A	**GPS L1C**	**Galileo E1 OS**
Non-coherent	106 sum. 106 ms	4 sum. 40 ms	12 sum. 48 ms
Coherent	24 ms	30 ms	24 ms

To study the impact of code Doppler on the acquisition performance; in the same conditions as previously presented, the probability of detection is computed considering Doppler and for the integration time described in Table VI. Let us remark that for GPS L5, the required total integration time to acquire at 27 dB•Hz exceeds the maximum total integration time before the slip of 1 chip. That means that if we want to acquire GPS L5, we suffer from the slip of 1 or 2 chips due to code Doppler.

When there is no Doppler, the probability of detection is around 0.9 but when an incoming Doppler is considered leading to a code Doppler, the probability of detection falls, particularly for non-coherent acquisition technique. The difference in acquisition performance between both acquisition accumulation techniques is mainly due to the integration time which is longer for non-coherent acquisition technique implying a higher offset between the incoming and the local spreading code sequence. The other argument is the better performance in terms of probability of detection for coherent accumulation. Of course, the higher the incoming Doppler frequency is, higher the degradations on the probability of detection are.

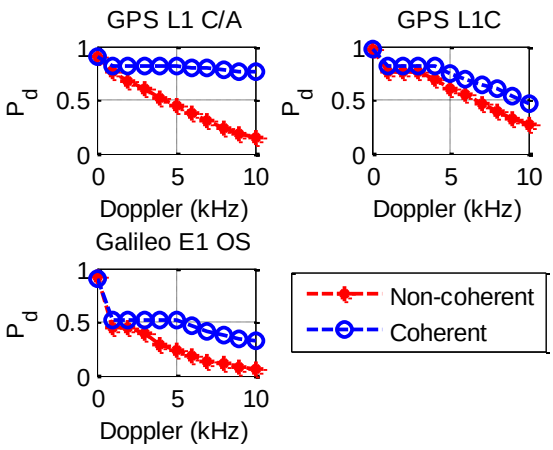

Figure 17: Probability of detection for the required acquisition time considering code Doppler (C/N_0 = 27 dB•Hz)

As previously explained in section I, the serial search acquisition is based on an acquisition grid. Herein, it is assumed that the acquisition is achieved which means that the bin corresponding to the right estimation of the incoming code delay and Doppler frequency is found. The point of interest is the incoming Doppler frequency for which the chip offset due to code Doppler leads to a change in the grid acquisition bin. In Figure 18, the position of the main peak of the resulting autocorrelation function is given for each integration on NT_c and for several incoming Doppler frequencies. This permits to understand the relationship between the Doppler frequency and the number of successive summation. For instance, for the GPS L5 signal, the 3 first autocorrelations functions have a code shift lower than 0.25 (threshold given in Figure 3) for an incoming Doppler of 10 kHz; for 4 kHz, the 8 first ones.

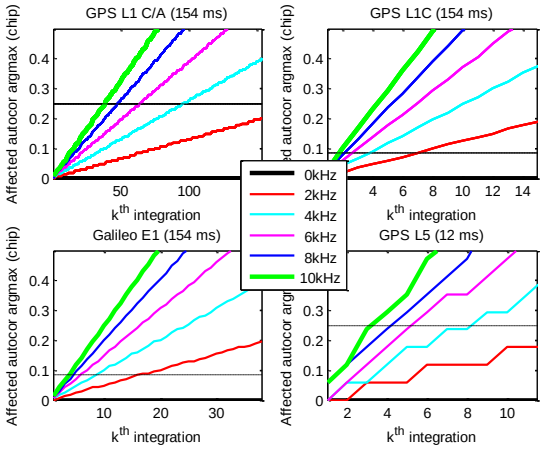

Figure 18: Probability of detection for the required acquisition time considering code Doppler (C/N_0 = 27 dB•Hz)

To complete this result, we are interested on the impact on the acquisition performance versus the acquisition accumulation technique (coherent or non-coherent). Table VII provides maximum Doppler frequency for which there is no acquisition grid cell change and this for all of the signals, acquisition techniques and K^{th} integration. Of course, an average process occurs leading to higher Doppler for coherent or non-coherent accumulation on KNT_c than the K^{th} integration. This means that for an incoming Doppler of 5 kHz (or less), the peak of the resulting non-coherent autocorrelation function is for a chip offset lower than 0.25 when the maximum integration time is processed (154 ms). It is clear that for BOC-modulated signals, the incoming Doppler frequency limit is low because of the strong code Doppler impact.

Table VII: Acquisition grid cell shift for the maximal integration time

	GPS L1 C/A	GPS L1C	Galileo E1 OS	GPS L5
K^{th} integration	3 kHz	1 kHz	1 kHz	3 kHz
Non-coherent	5 kHz	2 kHz	2 kHz	2 kHz
Coherent	6 kHz	1 kHz	2 kHz	4 kHz

We concluded that the coherent accumulation provides better acquisition performances (in terms of probability of detection) even if the losses on the autocorrelation peak amplitude are higher.

IV. CODE DOPPLER COMPENSATION METHODS

In the previous sections, the impact of the code Doppler on the acquisition performance has been demonstrated highlighting:

- The higher the incoming Doppler frequency is, the higher the losses are
- The weaker the signal is, the higher the losses are

So, now, knowing that, a state-of-the-art of the code Doppler compensation acquisition method is proposed.

Code Doppler compensation on the spreading code sequences

1) Local code generation based on the incoming Doppler

The first code compensation method is the simplest one and is proposed in [19] for the Double Block Zero Padding (DBZP) which algorithm steps are presented in [20]. It consists in generating for each possible incoming Doppler frequency a local version of the spreading code which code rate depends on the estimate of the Doppler frequency. Then, there are as many replica code versions as there are cells in the acquisition grid in the frequency search space. The ith local code version is used for the calculation of the coherent integration of the ith Doppler frequency estimate. Only the coherent result which is maximum (and corresponds to the right estimation of the incoming code Doppler) is kept.

This computational analysis of this method brings to the conclusion that it is very expensive in terms of number of computations and storage space.

2) Interpolation

This code Doppler compensation method is based on a modification of the local code and was developed in [17]. In this method, the local code is generated in much the same way as for classical acquisition method, in that the code frequency is varied with the Doppler frequency estimate. Then, for every Doppler frequency estimate, an interpolation of both the received signal and the local one is performed to ensure that there is exactly one full spreading code period of each present in the coherent integration interval.
This method permits to provide code Doppler compensation within and between coherent integration intervals but requires large memory due to the storage of the sampled local codes.

3) Time shift theorem implementation

The time shift-theorem can be applied to achieve Doppler code compensation. Indeed, the time-shift frequency theorem is:

$$\mathcal{F}\big(f(t+\tau)\big)(\zeta) = \exp(i\zeta\tau)F(\zeta) \qquad (27)$$

Where

- $\mathcal{F}$ is the Fourier transform operator
- f is a function
- F is the Fourier transform of f

Then, for FFT-based acquisition method, the code delay induced by code Doppler can be compensated by multiplying in the frequency domain the FFT of the local spreading code by the complex exponential $\exp\left(-i \times k\frac{\widehat{f_d}}{f_L}\right)$. This technique was patented by Krasner [21] and also applied in [22] which proposes an illustration given in Figure 19.

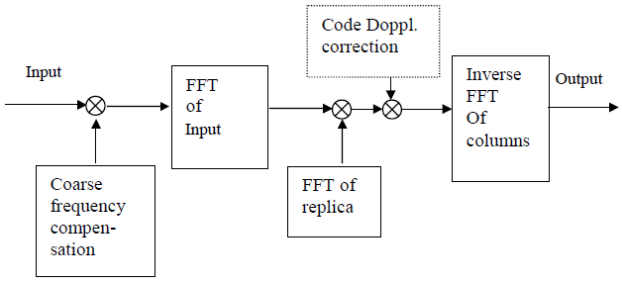

Figure 19: Krasner' technique [22]

The advantage of this method is that if the Fourier transform of the spreading code sequence has been built and stored in the memory, then the Fourier transform of the receded (or extended) spreading code can be transformed to the frequency domain in a simple way. Then the correct spreading code can be produced quickly. It can be seen as read more or less quick the stocked local spreading codes.

Code Doppler compensation on the correlator outputs

This method which is based on code Doppler picking points compensation is presented in [3] and consists in picking points in coherent integration results to compensate phase sliding. It is illustrated by Figure 20. The estimation of the code Doppler (depending on the incoming Doppler frequency) permits to calculate the code phase shift moments to compensate phase sliding. The coherent summation results should compensate the chip offset to guarantee all of the correlation peaks appear in unique code phase.

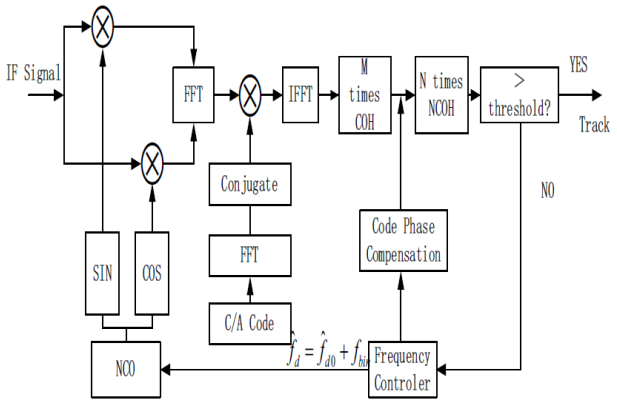

Figure 20: Code Doppler picking points compensation method [3]

This method provides improvements in acquisition performance by still calculating the correct code phase even in more extreme environment. Based on fast Fourier transform, this method does not require important resource consumptions and storage.

CONCLUSION

In this paper, a study on the code Doppler impact on the acquisition performance of new GNSS signals was presented. To conclude it, we will summarize the main results.
A first theoretic result gives the maximum total integration time before the slip between local and received sequences of 1 chip. To keep in mind is that for GPS L1 C/A, Galileo E1 OS and GPS L1C which share the same L-band, it is 154 ms for an incoming Doppler frequency of 10 kHz. Then, for GPS and Galileo signals in the L5 band and GPS L1C, one cannot sum more than 15 spreading codes for a 10 kHz incoming Doppler frequency if he does not want to suffer from 1-chip slip.
The autocorrelation function affected by code Doppler is significantly degraded: rounded and offset. Due to BOC modulation, Galileo E1 OS and GPS L1C present more degradation on the peak amplitude than BPSK-modulated signals. The phenomenon is particularly visible for coherent accumulation rather than non-coherent accumulation. However, the coherent accumulation technique presents less acquisition degradations in terms of probability of detection.
Finally, the degradations on the acquisition performance are considerable when weak signals should be acquired due to the long required integration time. Once again, the non-coherent accumulation technique suffers more than coherent accumulation when dealing with the probability of detection.

As it has been explained, for the new challenges (low C/N_0 environments, new GNSS signal structures, new applications…), one can hardly assume that there is no code Doppler. One possibility is to consider code Doppler compensation methods which are developed to limit acquisition performance losses when considering code Doppler. Maybe, some new code Doppler compensation methods can be explored to specific uses in terms of signal structures and sensitivity. Anyway, the residual losses when using these code Doppler compensation methods should be explained to permit to understand how these methods can be applied for the acquisition process.

REFERENCES

[1] J. K. Holmes, *Coherent Spread Spectrum systems*, New-York Wiley. 1982.

[2] U. Cheng, W. J. Hurd, and J. I. Statman, "Spread-Spectrum Code Acquisition in the Presence of Doppler Shift and Data Modulation," *IEEE Trans. Commun.*, vol. 28, no. 2, Feb. 1990.

[3] X. Jiao, J. Wang, and X. Li, "High Sensitivity GPS Acquisition Algorithm Based on Code Doppler Compensation," in *11th International Conference on Signal Processing (ICSP)*, Beijing, China, 2012.

[4] F. S. T. Van Diggelen, *A-GPS assisted GPS, GNSS, and SBAS*. Boston: Artech House, 2009.

[5] European Union, "European GNSS (Galileo) Open Service Signal In Space Interface Control Document." Feb-2010.

[6] M. Foucras, O. Julien, C. Macabiau, and B. Ekambi, "An Efficient Strategy for the Acquisition of Weak Galileo E1 OS Signals," in *ENC GNSS 2013*, Vienna, Austria, 2013.

[7] J. A. Avila-Rodriguez, "On Generalized Signal Waveforms for Satellite Navigation," PhD, Munich, Germany, 2008.

[8] Navstar, "Navstar Global Positioning System GPS Space Segment / Navigation User Interfaces." Dec-2004.

[9] Navstar, "Global Positioning Systems Directorate Systems Engineering & Integration Interface Specification IS-GPS-800 navstar GPS Space Segment/User Segment L1C Interface." 05-Sep-2012.

[10] Navstar, "Global Postioning Systems Directorate Systems Engineering & Integration Interface Specification IS-GPS-705 Navstar GPS Space Segment/User Segment L5 Interfaces." 05-Sep-2012.

[11] H. Al Bitar, "Advanced GPS signal processing techniques for LBS services," PhD, Institut National Polytechnique de Toulouse, ENAC, Toulouse, France, 2007.

[12] RTCA, Inc, "Assessment of Radio Frequency Interference Relevant to the GNSS L1 Frequency Band RTCA/DO-235B." 13-Mar-2008.

[13] F. Bastide, O. Julien, C. Macabiau, and B. Roturier, "Analysis of L5/E5 Acquisition, Tracking and Data Demodulation Thresholds," in *ION GPS 2002*, Portland, OR, 2002.

[14] D. Lin and J. B. Y. Tsui, "Comparison of acquisition methods for software GPS receiver," in *ION GPS 2000*, Salt Lake City, UT, 2000, pp. 19–22.

[15] J. B.-Y. Tsui, *Fundamentals of Global Positioning System Receivers: A Software Approach*, Wiley Series in Microwave and Optical Engineering. Wiley Series in Microwave and Optical Engineering, 2004.

[16] C. O'Driscoll, "Performance analysis of the parallel acquisition of weak GPS signals," PhD, National University of Ireland, National University of Ireland, 2007.

[17] M. L. Psiaki, "Block Acquisition of Weak GPS Signals in a Software Receiver," in *14th International Technical Meeting of the Satellite Divsion of The Institute of Navigation*, Salt Lake City, UT, 2001, pp. 11–14.

[18] F. Bastide, "Analysis of the Feasibility and Interests of Galileo E5a/E5b and GPS L5 for Use with Civil Aviation," PhD, Institut National Polytechnique de Toulouse, ENAC, Toulouse, France, 2004.

[19] N. I. Ziedan, *GNSS receivers for weak signals*, Artech House. Artech House, 2006.

[20] M. Foucras, O. Julien, C. Macabiau, and B. Ekambi, "A Novel Computationally Efficient Galileo E1 OS Acquisition Method for GNSS Software Receiver," in *25th International Technical Meeting of the Satellite Division of The Institute of Navigation*, Nashville, TN, 2012.

[21] N. F. Krasner, "GPS Receiver and Method for Processing GPS Signals," 5,781,156Jul-1998.

[22] D. Akopian, "A Fast Satellite Acquisition Method," in *ION GPS 2001*, Salt Lake City, UT, 2001.